Available online at www.sciencedirect.com
SCIENCE DIRECT®
Journal of Nuclear Materials 347 (2005) 88–93
journal of nuclear materials
www.elsevier.com/locate/jnucmat

Colloids from the aqueous corrosion of aluminium-based nuclear fuel

M.D. Kaminski *, M.M. Goldberg, C.J. Mertz

Argonne National Laboratory, Chemical Engineering Division, 9700 South Cass Avenue, Argonne, IL 60439, USA

Received 3 March 2005; accepted 21 July 2005

Abstract

Nuclear wastes to be buried in the proposed repository underneath Yucca Mountain, Nevada, may produce colloids and contribute to the release of radioactivity from the repository. As a component of non-commercial nuclear fuels slated for disposal, aluminium-based fuels may release the colloids during aqueous corrosion. This paper reports on the characterization of such colloids, which are predominantly clays >100 nm. Colloid concentrations never exceeded 8×10^{11} particles/L, which is well within the range of values used in the repository release models. These colloids carry 99% of the released uranium and highlight the potential importance of the colloid phase in determining radionuclide transport from the uranium–aluminium fuels.

PACS: 28.41.Kw

1. Introduction

As part of an environmental assessment of a geologic repository for high-level radioactive waste and spent nuclear fuel, the US Department of Energy (DoE) models radioactivity release from the waste package and subsequent transport through the subsurface. Radioactive colloids generated during the corrosion of the waste represent potentially important sources of radioactive release, yet they are incompletely identified and poorly understood. This knowledge gap propagates into large uncertainties in predictive-model release calculations and was cited as a deficiency by expert evaluation of US efforts in this area [1].

To date, information has appeared in the literature on the nature of the colloids formed during the oxidative corrosion of high-level waste glass [2–6] and references therein] and commercial uranium oxide (UO_2) fuels [7]. Fortner et al. [8] describe colloids generated during the corrosion of production reactor fuel owned by the DoE. Still, none of the more than 200 other fuel types in the DoE inventory has been characterized for colloid production and reported in the peer-review literature. As one of the fuels chosen by the DoE for evaluation, aluminium-based spent nuclear fuels represent a potentially significant component of the inventory, due to their high fissile uranium concentration, relative volume in the DoE inventory, and high fission and activation product concentration resulting from high burnup. We focused our research on colloids produced during the aqueous

* Corresponding author. Tel.: +1 630 252 4777; fax: +1 630 252 4771/5246.
E-mail address: kaminski@cmt.anl.gov (M.D. Kaminski).

0022-3115/$ - see front matter © 2005 Elsevier B.V. All rights reserved.
doi:10.1016/j.jnucmat.2005.07.010

corrosion of aluminium-based nuclear fuel. In this paper, we determine the concentration, size distribution, and morphology of the colloids and discuss the significance of this data to the repository.

2. Experimental

2.1. Materials and testing

The well water was prepared from water sampled from the J-13 well near Yucca Mountain and modified with volcanic detritus or tuff that characterizes the geology of Yucca Mountain, as described in [9]. The ionic strength and pH of the modified water was ~3 millimolal and 7–8, respectively (within the stability regime for montmorillonite clay [2]). The cation concentrations (μg/g or ppm) in the modified groundwater (herein referred to as 'well water') were Na: 70–707, Mg: 0.01–0.21, Al: 0.11–1.36, Si: 27–144, Ca: 2.4–10.1, Fe: 0.01–1.82, U: 0.0008–0.1.

The test scheme was designed to observe colloidal products as a result of direct colloid production (e.g., spallation of oxidized fuel products in the colloidal size range) and that from the precipitation of material (colloidal precipitates formed when the solubility product was exceeded). We dripped well water intermittently (0.75 mL twice weekly) onto the face of a non-radiated uranium aluminide fuel coupon ($5 \times 4 \times 2$ mm, see Table 1) placed horizontally inside a perforated Zircaloy cup that was suspended inside a stainless steel test vessel. The water drained off the fuel and passed through a series of gold mesh sieves with 11 μm openings and larger (to trap particulates) and into the base of the sealed vessel. We ran three tests of varied duration at 90 °C (Test 1 = 16 days, Test 2 = 55 days, Test 3 = 183 days). Periodically, we cooled the vessel to room temperature and withdrew all of the reacted well water from the base for analysis. Control tests containing no fuel were run concurrently and analyzed after 83 and 151 days.

Table 1
Composition of U–Al fuel

Element	Fuel meat (g/g)	Cladding (g/g)
Na	2.92×10^{-5}	$<4 \times 10^{-4}$
Mg	2.63×10^{-5}	3.13×10^{-2}
Al	0.497	9.62×10^{-1}
Si	2.5×10^{-4}	3.06×10^{-4}
K	9.74×10^{-5}	1.61×10^{-4}
Ca	3.9×10^{-4}	8.41×10^{-4}
Fe	1.45×10^{-3}	3.44×10^{-3}
Zr	1.45×10^{-5}	8.66×10^{-6}
Au	9.68×10^{-8}	1.93×10^{-7}
^{235}U	0.10	NA
^{238}U	0.39	4.07×10^{-5}
Total	0.99	1.0

2.2. Analysis

The concentration of metals in the reacted well water (or leachate) at the base of the vessel that passed through a 30 kDa filter (Millipore-Ultrafree MC) represented the dissolved fraction. This number was subtracted from the unfiltered leachate concentrations (colloidal/particulate <11 μm + dissolved) to determine the colloidal/particulate fraction. Liquid samples were acidified and analyzed by inductively coupled plasma mass spectrometry, as described elsewhere [10].

Transmission electron microscopy (acc. voltage = 200 kV) and energy dispersive X-ray analysis were used to characterize the morphology and composition of colloids prepared by passing unfiltered sample leachate through a Formvar-coated grid (Ladd Research) or a hydrophilic Butvar-coated grid prepared in-house.

Dynamic laser light scattering was used to determine the concentration and size distribution of the colloids using an argon ion laser at 3–20 mW (Malvern PCS4700C, 515 nm, 500 μm PMT aperture). Samples consisting of approximately 400 μL of unfiltered leachate were stored in cylindrical glass vials at room temperature. We analyzed samples withdrawn at the end of three tests (day 16 for Test 1, day 55 for Test 2, and day 183 for Test 3) at various times after test termination to monitor the effect of storage time on scattering intensity. Precipitates that formed after prolonged storage were removed by centrifugation prior to analysis of the solution. Scattering intensities were measured at an angle of 90°. The unit was checked against polystyrene standards from Duke Scientific (33, 73, 304 nm diameters) and NIST (SRM 1963 and SRM 1691, 100 and 269 nm diameters, respectively) for size agreement. Bimodal standards prepared from 32 and 100 nm standards confirmed the deconvolution of discrete colloid populations. The CONTIN [11] inversion program calculated colloid size distributions based on temporal fluctuations in light scattering intensity.

Average light scattering intensities were correlated with particle concentrations by assuming that light scattering intensities measured at 3 mW for the standard spheres and unknown samples are similar for identical concentrations. The measured intensities produced curves from which concentrations of unknown samples were estimated (Fig. 1). This is an acceptable method of estimation if the unknown colloids are spherical and the refractive index of the standards ($n_{RI} = 1.6$) is near that of the unknown [12]. As will be shown, clays have a refractive index similar to the standards ($n_{RI} = 1.53$–1.64), comprised a significant fraction of the colloids, and the aggregates were roughly spherical, thus lending credence to this method of estimation.

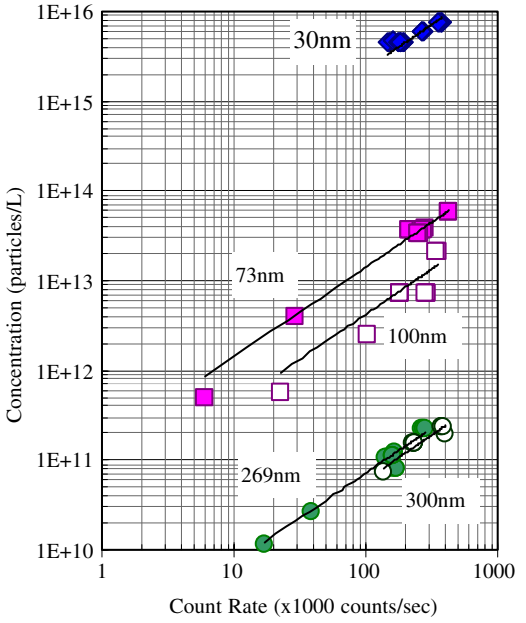

Fig. 1. Polystyrene number concentrations associated with light scattering intensities (count rate; $\times 10^3$ counts per sec, or kcps). The lines are linear fits of the data.

3. Results

Light scattering intensities revealed significant colloid concentrations in each of the samples analyzed (Fig. 2). Compared to the well water stock (<7 kcps), the measured values (15–69 kcps) exceeded the stock for all samples and periods analyzed. During the storage period, light scattering intensities decreased, indicating a decrease in colloid concentration. This is consistent with the precipitates visible in the sample vial after prolonged storage. The control tests containing no fuel also produced slightly elevated scattering intensities (10–16 kcps), indicating that well water alone can nucleate colloids under these test conditions.

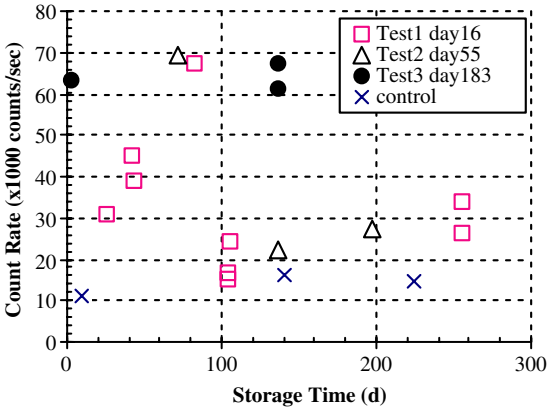

Fig. 2. Light scattering intensity (count rate in kcps) for UAl_x leachate samples during sample storage.

Light scattering analysis from the three fuel tests indicated broad colloidal size distributions. The polydispersity indices, σ ($0 \leqslant \sigma \leqslant 1$), are related to the variances of the size distribution peaks, and were 0.6 ± 0.2 (number of measurements, $n = 24$) for Test 1, 0.4 ± 0.2 ($n = 30$) for Test 2, and 0.7 ± 0.3 ($n = 21$) for Test 3. In general, these large σ values prohibit precise size distribution calculations. This was apparent during most sample analyses where very few analysis trials converged on a single solution. Instead, the software determined a broad, often bimodal size distribution ($d < 10$ nm, $d > 100$ nm). We chose to ignore the small size because of the lack of microscopic evidence substantiating the existence of colloids at that size. The mean diameters were 260 ± 20 nm (Test 2, day 16) and 140 ± 30 nm (Test 3, day 183).

Based on the estimated mean diameter, the scattering intensity (count rate) shown in Fig. 2, and the correlation of particle size, concentration and scattering intensity shown in Fig. 1, we estimated the particle concentrations of the colloids. For test 2, day 16, with a scattering intensity of 15–69 kcps and a mean diameter of 260 ± 20 nm diameter, the estimated colloid concentration is $<10^{10}$–5×10^{10} particles/L using the 269 nm size. For Test 3, day 183, with scattering intensity of 62 ± 5 kcps and a mean diameter of 140 ± 30 nm, the colloid concentration, estimated using a 100 nm diameter standard, is 2×10^{12} particles/L, and using a 300 nm diameter is 4×10^{10} particles/L. To extrapolate to 140 nm we use the relation

$$\log(C) = m \log(r^{-6}) + b, \tag{1}$$

where C is concentration of colloids in particles/L and r is the radius in nm and m and b are the slope and intercept of the constant count rate line through the 73, 100, 269, and 300 nm standards in Fig. 1. This equation is valid for colloids of the same substrate and morphology at a constant light scattering intensity. Using this method yields a concentration of 8×10^{11} particles/L for 140 nm colloids.

X-ray analysis under the electron microscope revealed silicon-rich and aluminium-rich colloidal aggregates whose elemental compositions were consistent with those of clays and aluminium hydroxide minerals. In general, the sizes and shapes of colloids varied greatly. Silica-rich colloids were prevalent in all samples (Fig. 3(a) and (b)). The silica-rich colloids were typically larger than a few hundred nanometers, varied in morphology, and contained P and K; aluminium was also observed frequently in the X-ray analysis. Colloids predominantly composed of aluminium and oxygen were much less prevalent (Fig. 3(c)) and contained small

amounts of Si, P, and Cl. The colloid shown in Fig. 3(d) appears to be an aggregate composed of many tiny colloids <10 nm in diameter.

Clays of similar morphology to smectites described by Buck and Bates [3], were found in larger flocs hundreds of nanometers to >1000 nm in size. X-ray analysis

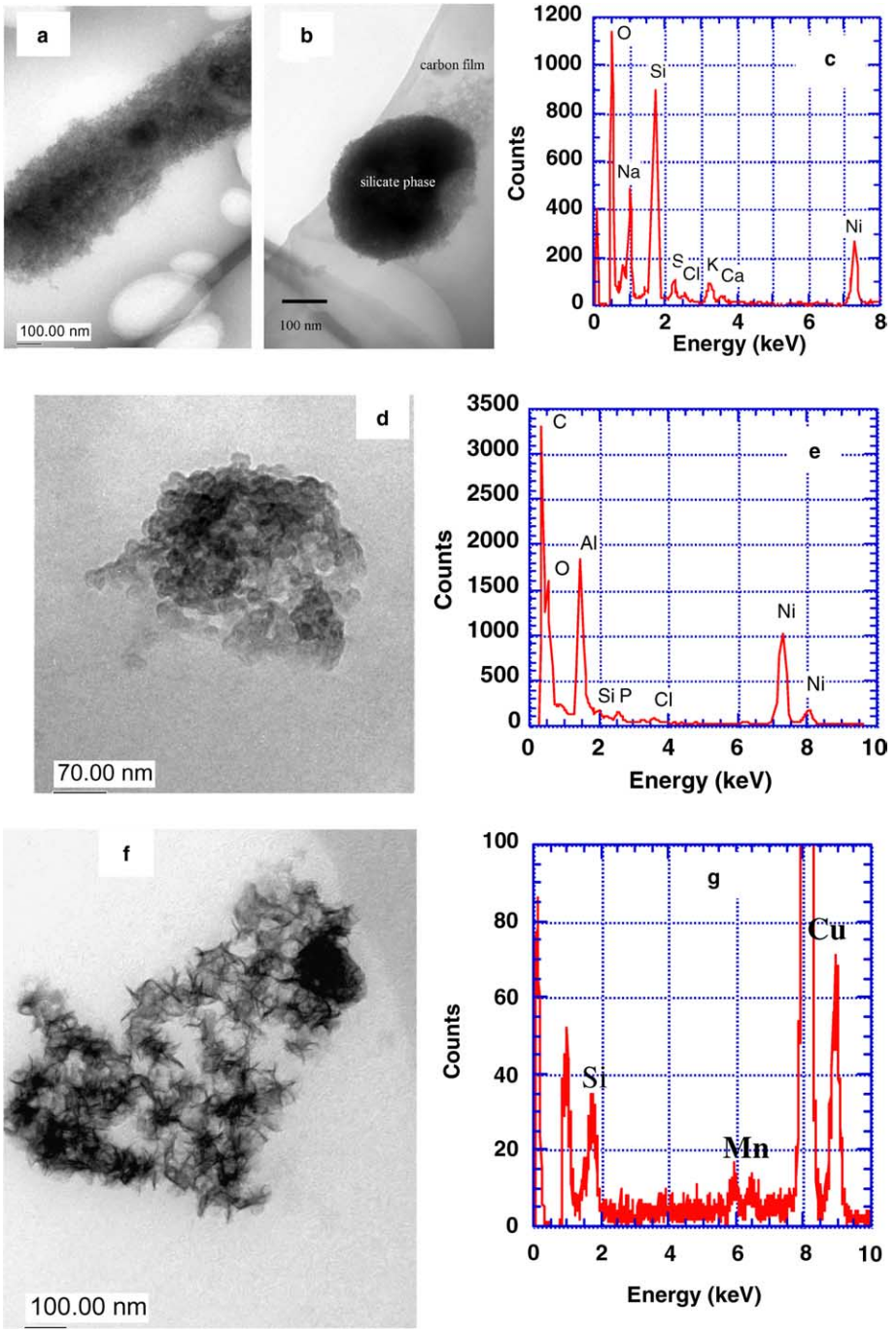

Fig. 3. TEM micrographs of silicate colloids (a,b) and typical X-ray spectrum (c); Al-oxide colloid aggregate (d) and X-ray spectrum (e) and aggregated smectite-type clay (f) and X-ray spectrum (g).

Table 2
Dissolved and colloidal/particulate concentrations (mg/L) for some clay-forming elements from Test 2 Day 16 (unfiltered and dissolved values carry a 10% error)

Element	Total	Dissolved	Colloidal/particulate	% Colloidal
Mg	0.13	0.079	0.048	40
Al	1.36	0.0062	1.35	~100
Si	43.1	32.4	10.7	25
Ca	6.1	6.9	0	0
U	0.10	0.0013	0.099	99

suggested that they were composed primarily of manganese and silicon but they were too thin to yield a reliable electron diffraction pattern. Iron-rich colloids were also identified and contained O, Si, Al, Mg, and K to varying degrees.

The filtration data presented in Table 2 was used to determine the bulk colloid composition and corroborates the microscopy data in suggesting clays. Except for Ca, the elements commonly found in clays, Mg, Al, and Si, constituted a significant fraction of the colloids (Table 2). Iron could not be determined in the clay fractions due to large elemental uncertainties. The lack of calcium associated with the colloidal range was surprising, since calcium is expected to adsorb strongly to clays and is a common interlayer cation in the smectite clays. The aluminium concentration is consistent with solubility control by poorly crystallized silicate clays (solubility limit = 0.006 mg/L at neutral pH) [13]. The dissolved silicon concentration is also within the range expected for solubility control by amorphous silicates [13]. Of particular importance to the repository is the strong association of uranium with the colloidal/particulate phase (99%).

4. Discussion

The colloid population appears to be predominantly smectite-type silicate-based clays. The origin of the silicon can be both the well water, which is silica saturated, and the fuel which contains silicon. The morphology shown in Fig. 3(d) is consistent with the description provided by Buck and Bates [3] but the presence of manganese, likely leached from the steel test vessel, in the sample is unusual for the smectites. There is also evidence from our laboratory that clays of similar morphology may contain nickel, another unusual element for natural systems but available in steels. Thus, we must conclude that these colloids differ from natural colloidal systems, and, due to the presence of manganese and other metals from the well water, may include these metals within the smectite structure. Some aluminium-rich colloids were observed.

Colloid size was diverse, and results from both microscopy (varied colloid aggregate size) and light scattering (large polydispersity indices) analyses agreed with each other. Colloid concentrations were estimated based on average diameters determined by light scattering – $<10^{10}$–5×10^{10} particles/L and 8×10^{11} particles/L. Both these values are well within the range accounted for by the repository models [2].

The colloids appear to originate from two sources. Since the control tests containing no fuel produced elevated scattering intensities, the well water alone will produce colloids under our test conditions, perhaps by providing nucleating metals from the corroding steel vessel. In the repository, corroding stainless steel waste packages will supply these same elements to the fuel corrosion products. The other source of colloids is the corrosion of the fuel. The aluminium-rich colloids are evidence of that. A study of aluminium fuel corrosion shows that a thin aluminium gel layer forms at the surface [8]. Peptization of the gel by dripping water may produce these aluminium oxide colloids [14]. In addition, colloids precipitate from solution with increasing ionic strength. They are often precipitated and flocculated in solution with aluminuim ions, a customary practice in water treatment, since their +3 charge greatly increases ionic strength and decreases the electric double layer protecting colloids from aggregation phenomena. Thus, we can expect that the prevalence of aluminium ions from the dissolution of Al-based fuels causes a dramatic increase in colloid and aggregated colloidal populations than if the fuel was absent.

The question of radionuclide association with these colloids is of paramount importance. Although these tests describe non-irradiated fuels, uranium behavior is instructive. Since we showed that the uranyl oxyhydroxides were formed immediately during the corrosion of the aluminium fuel [8], we can confidently assign the hexavalent oxidation state to the uranium released into the groundwater leachate. Uranyl ions (UO_2^{2+}) can bind strongly to clays (see Table 4 in Ref. [2]). Our filtration data supports this by showing that uranium is almost exclusively associated with the colloidal/particulate fraction. However, for repository performance, uranium is not considered a main contributor to the potential dose. Instead, the transuranium actinides are important, particularly Np, Pu, and Am. In 'burned' aluminium fuels, the actinide inventory is far greater, on average, than for commercial spent fuels. This is due to higher fuel enrichment (13–93% ^{235}U, compared to 3% in commercial reactor fuel) and extremely high burnups[1] (>50%

[1] Burnup, or more correctly, fractional burnup, describes the fraction of energy released from the fuel for a given mass of fuel. A burnup of 100% would completely consume all fissionable isotopes in the fuel.

burnup in many types, compared to 3% for commercial fuel). The environmental chemistry of the actinides teaches that Np will exist as Np(V), Pu as Pu(IV,VI), and Am as Am(III) in various hydrated or oxo-species [2]. These species have been clearly identified as strongly adsorbable to clay surfaces [2]. Thus, we can expect colloids to play an important role in the disposition of the actinide inventory from aluminium fuels. However, the small inventory of aluminium fuels (0.012% of total fuel slated for the repository [1]) combined with our estimated concentration of colloids and radioactivity associated with them greatly lessen the potential impact the colloids may have on the performance of the repository as a whole.

5. Conclusions

These data are insufficient for predicting the true impact of the colloids identified in this study on radionuclide transport from the repository. Indeed, the stability of the colloids against precipitation/agglomeration or dissolution has not been sufficiently studied, nor has their subsurface transport characteristics been evaluated. Both stability and transport of colloids are extremely complicated phenomena, but understanding them is crucial for properly assessing the long-term viability of a repository. Moreover, potential effects of abrupt temperature changes (such as those experienced in this study) on colloid formation have not been investigated. Nevertheless, our results are useful to performance assessment modelers because the colloid concentration data *do* conform to the range of values already used as input into the repository release models and reveal for the first time the varied composition and morphology of colloids formed when well water reacts with aluminium-based nuclear fuel.

Acknowledgements

The authors thank J. Emery and M. Clark for assistance with experimental setup and J. Holly for assistance with the TEM. Work is supported by the US Department of Energy, Office of Environmental Management under guidance of the National Spent Nuclear Fuel Program, under Contract Number W-31-109-ENG-38.

References

[1] Final Report Total System Performance Assessment Peer Review Panel, Feb. 11, 1999, p. 96.
[2] R. Aguilar, Waste Form Colloid-Associated Concentration Limits: Abstraction and Summary, ANL-WIS-MD-000012 REV00 ICN01, December 2000.
[3] E.C. Buck, J.K. Bates, Appl. Geochem. 14 (1999) 635.
[4] J.K. Bates, J.P. Bradley, A. Teetsov, C.R. Bradley, M. Buchholtz ten Brink, Science 256 (1992) 649.
[5] W.L. Ebert, J.K. Bates, Nucl. Technol. 104 (1993) 372.
[6] H. Geckeis, B. Grambow, A. Loida, B. Luckscheiter, E. Smailos, J. Quinones, Radiochim. Acta 82 (1998) 123.
[7] P.A. Finn, E.C. Buck, M. Gong, J.C. Hoh, J.W. Emery, L.D. Hafenrichter, J.K. Bates, Radiochim. Acta 66&67 (1994) 189.
[8] J.A. Fortner, C.J. Mertz, M.M. Goldberg, S. Seifert, in: American Nuclear Society Fifth Topical Meeting on DOE Spent Fuel and Fissile Materials Management, Charleston, SC, 17–20 September 2002.
[9] M.D. Kaminski, M.M. Goldberg, J. Nucl. Mater. 304 (2002) 182.
[10] S.F. Wolf, J. Radioanal. Nucl. Chem. 235 (1998) 207.
[11] S.W. Provencher, Comput. Phys. Commun. 27 (1982) 213.
[12] P. Schurtenberger, M.E. Newman, Environmental Particles, Environmental Analytical and Physical Chemistry Series, 2, Lewis Publishers, Ann Arbor, 1993, p. 95.
[13] J.D. Hem, USGS Water Supply Paper 2254, United States Government Printing Office, Washington, DC, 1992, p. 75.
[14] C.J. Plank, J. Colloid Sci. (1947) 413.